Reproducibility of Complex Turbulent Flow Using Commercially-Available CFD Software
—Report 3: For the Case of a Three-dimensional Cube—

Takanori UCHIDA[*1]

E-mail of corresponding author: *takanori@riam.kyushu-u.ac.jp*

(Received January 29, 2016)

Abstract

Choosing appropriate sites for wind turbines is extremely important in Japan because the spatial distribution of wind speed is highly complex over steep complex terrain, which is abundant in Japan. The author's research group has been developing an unsteady CFD software package called RIAM-COMPACT®. This package is based on an LES turbulence model. In this paper, to examine the accuracy of RIAM-COMPACT®, numerical simulations of uniform, non-stratified airflow past a three-dimensional cube were performed. The analysis primarily focused on airflow characteristics in the wake region. The results from the simulation with RIAM-COMPACT® were compared to those from a commercially-available CFD software package (STAR-CCM+) and were found to be in good agreement.

Key words: *Commercially-available CFD software, STAR-CCM+, RIAM-COMPACT®, Cube model*

1. Introduction

The author's research group has developed the numerical wind diagnosis technique named RIAM-COMPACT® [1,2]. The core technology of RIAM-COMPACT® is under continuous development at the Research Institute for Applied Mechanics, Kyushu University, Japan. An exclusive license of the core technology has been granted by Kyushu TLO Co., Ltd. (Kyushu University TLO) to RIAM-COMPACT Co., Ltd. (http://www.riam-compact.com/), a venture corporation which was founded by the author and originated at Kyushu University in 2006. A trademark, RIAM-COMPACT®, and a utility model patent were granted to RIAM-COMPACT Co., Ltd. in the same year. In the meantime, a software package has been developed based on the above-mentioned technique and is named the RIAM-COMPACT® natural terrain version software. Efforts have been made to promote this software as a standard software package in the wind power industry.

In the previous paper [1,2], a numerical simulation was performed for airflow around an isolated-hill with a steep slope angle using RIAM-COMPACT® natural terrain version, and the results were compared to those from numerical simulations performed using another commercially-available CFD software package.

In the present paper, a similar study is conducted for airflow around a three-dimensional cube, and the results of the comparisons are discussed.

2. Summary of Commercially-Available CFD Software

Commercially-available computational fluid dynamics (CFD) software packages have been developed and used mainly as design tools primarily in the automobile and aviation industries up to the present time. The following is a list of the major CFD software packages available on the market:

General-purpose CFD thermal fluid analysis software packages

■STAR-CCM+
http://www.cd-adapco.co.jp/products/star_ccm_plus/index.html

■ANSYS(CFD, Fluent, CFX)
http://ansys.jp/solutions/analysis/fluid/index.html

■SCRYU/Tetra
http://www.cradle.co.jp/products/scryutetra/

■STREAM
http://www.cradle.co.jp/products/stream/index.html

■CFD2000
http://www.cae-sc.jp/docs/cfd2000/index.htm

*1 Research Institute for Applied Mechanics, Kyushu University

■PHOENICS
http://www.phoenics.co.jp/

■Autodesk Simulation CFD
http://www.cfdesign.com/

■CFD++
http://bakuhatsu.jp/software/cfd/

■CFD-ACE+
http://www.wavefront.co.jp/CAE/cfd-ace-plus/

■AcuSolve
http://acusolve.jsol.co.jp/index.html

■FLOW-3D
http://www.terrabyte.co.jp/FLOW-3D/flow3d.htm

■FloEFD
http://www.sbd.jp/product/netsu/floefd3cad.shtml

■Flow Designer
http://www.akl.co.jp/

■PowerFLOW
http://www.exajapan.jp/pages/products/pflow_main.html

■KeyFlow
http://www.kagiken.co.jp/product/keyflow/index.shtml

■OpenFOAM
http://www.cae-sc.jp/docs/FOAM/

■FrontFlow
http://www.advancesoft.jp/product/advance_frontflow_red/

The wind power industry has independently developed and distributed CFD software designed for selecting sites appropriate for the installation of wind turbines (see the list below). Recently, some of the above-listed general-purpose thermal fluid analysis software packages have also started being adopted in the wind power industry.

CFD software packages designed for the wind power industry (wind farm design tools)

■RIAM-COMPACT®
http://www.riam-compact.com/

■MASCOT
http://aquanet21.ddo.jp/mascot/

■WindSim
http://www.windsim.com/

■METEODYN
http://meteodyn.com/

In the present paper, the simulation results from RIAM-COMPACT® natural terrain version are compared to those from STAR-CCM+, one of the leading commercially-available CFD software packages. The results of the comparison are discussed.

3. Summary of STAR-CCM+ Software

In this section, a summary of STAR-CCM+, a general-purpose thermal fluid analysis software package distributed by CD-adapco is provided (see Table 1). The version of the software package used in the present study is 8.02.008 (for 64-bit Windows).

STAR-CCM+ uses a single graphical user interface (GUI) for computational grid generation, execution of fluid analyses, and data post-processing. The grid generation method in STAR-CCM+ is distinctive. In STAR-CCM+, both a polyhedral grid and a prism layer grid can be used (for example, see Fig.3). The polyhedral grid is a new type of grid offered and promoted by CD-adapco and consists of polyhedral cells which possess 10 to 15 faces on average. The use of this cell type makes it possible to dramatically reduce 1) the number of grid cells required to obtain analysis results equivalent to those that can be obtained using a conventional tetrahedral grid and 2) the memory required by the solver. With the use of this cell type, the computational stability improves significantly, and the time required to obtain convergent solutions also decreases. The prism layer grid is a refined grid designed to capture the behavior of the boundary layer that develops over the surface of an object. In this type of grid, layers of thin grid cells are distributed regularly over the object. Since the thickness and number of layers in the normal direction with respect to the object surface can be freely adjusted, the behavior of the boundary layer in the vicinity of a wall can be captured with high accuracy. However, when the number of prism layer grid cells is very large, the computation time increases significantly.

Numerical simulations are based on the finite-volume method (FVM), and the Navier-Stokes equation is used as the governing equation. Iterative calculations are performed for the velocity and pressure fields using an algebraic multi-grid (AMG) linear solver. For the time marching method, a first-order implicit method is used. STAR-CCM+ can be run either with a Reynolds-averaged Navier-Stokes (RANS) turbulence model or a large-eddy simulation (LES) turbulence model. For the convective term in the RANS models, a second-order upwind scheme is adopted. For the convective term in the LES models, a bounded central differencing (BCD) scheme is employed. Table 1 shows an overview of the computational techniques, parameters, and simulation set-up used for one of the simulations performed with STAR-CCM+ in the present study, namely the simulation with a steady RANS turbulence model, as an example.

Simulation code	STAR-CCM+ v.8.02.008
Governing equation	Three-dimensional unsteady Navier-Stokes equation
Turbulence model	Steady RANS (Spalart-Allmaras one-equation eddy-viscosity turbulence model)
Time marching	1. First-order implicit unsteady analysis 2. Steady analysis (The steady-state solution is obtained by specifying the number of time steps.)
Duration of simulation	1. Spin-up: 0 - 100s in non-dimensional time (Time averaging: 100 - 200s in non-dimensional time) 2. Spin-up: 0 - 2000 in time step number (Time averaging: 2000 - 4000 in time step number)
Discretization of the convective term	A second-order upwind scheme (No options available other than first-order and second-order upwind schemes)
Gas	Constant density
Density ρ	1.0 [kg/m^3]

Coefficient of viscosity μ	1.0×10^{-5} [Pa•s]
Cube model height h	0.1 [m]
Inflow wind velocity U	1.0 [m/s]
Reynolds number $= U\,h\,(\rho / \mu) = U\,h\, / \,\nu$	1.0×10^4
Non-dimensional time step $\Delta t = (\Delta t\ U) / h$	2.5×10^{-2}
Number of grid cells	Approx. 1.06 million

Table 1 Overview of STAR-CCM+, for the case of the simulation using a steady RANS model in the present study

4. Summary of RIAM-COMPACT® Software

In this section, a summary of RIAM-COMPACT® natural terrain version, developed by the author's research group, will be described. In this software package, a collocated grid in a general curvilinear coordinate system is adopted in order to numerically predict local wind flow over complex terrain with high accuracy while avoiding numerical instability. In this collocated grid, the velocity components and pressure are defined at the grid cell centers, and variables that result from multiplying the contravariant velocity components by the Jacobian are defined at the cell faces. The numerical technique is based on the finite-difference method (FDM), and an LES model is adopted for the turbulence model. In the LES model, a spatial filter is applied to the flow field to separate eddies of various scales into grid-scale (GS) components, which are larger than the computational grid cells, and sub-grid scale (SGS) components, which are smaller than the computational grid cells. Large-scale eddies, i.e., the GS components of turbulence eddies, are directly numerically simulated without the use of a physically simplified model. In contrast, dissipation of energy, which is the main effect of small-scale eddies, i.e., the SGS components, is modeled according to a physics-based analysis of the SGS stress.

For the governing equations of the flow, a spatially-filtered continuity equation for incompressible fluid (Eq.(1)) and a spatially-filtered Navier-Stokes equation (Eq.(2)) are used.

$$\frac{\partial \bar{u}_i}{\partial x_i} = 0 \qquad -(1)$$

$$\frac{\partial \bar{u}_i}{\partial t} + \bar{u}_j \frac{\partial \bar{u}_i}{\partial x_j} = -\frac{\partial \bar{p}}{\partial x_i} + \frac{1}{Re}\frac{\partial^2 \bar{u}_i}{\partial x_j \partial x_j} - \frac{\partial \tau_{ij}}{\partial x_j} \qquad -(2)$$

$$\tau_{ij} \approx \overline{u_i' u_j'} \approx \frac{1}{3}\overline{u_k' u_k'}\delta_{ij} - 2\nu_{SGS}\bar{S}_{ij} \qquad -(3)$$

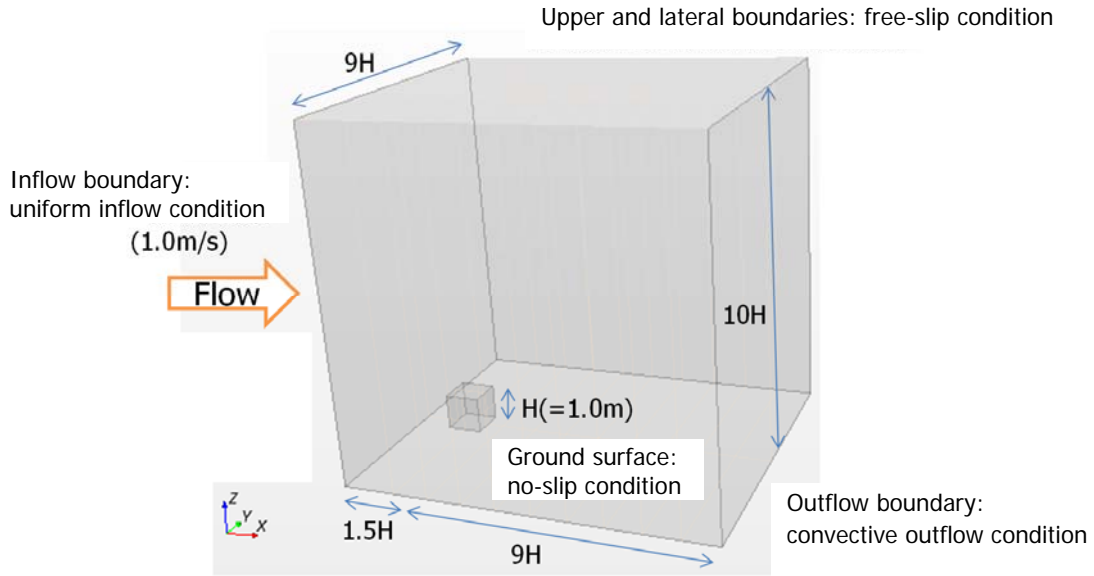Fig.1 Computational domain, coordinate system, boundary conditions, and other related information

$$\nu_{SGS} = \left(C_s f_s \Delta\right)^2 \left|\overline{S}\right| \qquad \text{-(4)}$$

$$\left|\overline{S}\right| = \left(2\overline{S}_{ij}\overline{S}_{ij}\right)^{1/2} \qquad \text{-(5)}$$

$$\overline{S}_{ij} = \frac{1}{2}\left(\frac{\partial \overline{u}_i}{\partial x_j} + \frac{\partial \overline{u}_j}{\partial x_i}\right) \qquad \text{-(6)}$$

$$f_s = 1 - \exp\left(-z^+ / 25\right) \qquad \text{-(7)}$$

$$\Delta = \left(h_x h_y h_z\right)^{1/3} \qquad \text{-(8)}$$

For the computational algorithm, a method similar to a fractional step (FS) method is used, and a time marching method based on the Euler explicit method is adopted. The Poisson's equation for pressure is solved by the successive over-relaxation (SOR) method. For discretization of all the spatial terms except for the convective term in Eq.(2), a second-order central difference scheme is applied. For the convective term, a third-order upwind difference scheme is applied. An interpolation technique based on four-point differencing and four-point interpolation by Kajishima is used for the fourth-order central differencing that appears in the discretized form of the convective term. For the weighting of the numerical diffusion term in the convective term discretized by third-order upwind differencing, $\alpha = 3.0$ is commonly applied in the Kawamura-Kuwahara scheme. However, $\alpha = 0.5$ is used in the present study to minimize the influence of numerical diffusion. For LES subgrid-scale modeling, the standard Smagorinsky model is adopted with a model coefficient of 0.1 in conjunction with a wall-damping function.

5. Flow Field and Simulation-setup Considered in the Present Study

In this section, the flow field, coordinate system, and simulation-setup considered for the present study are described (Fig.1).

For the boundary conditions, uniform inflow conditions, free-slip conditions, and convective outflow conditions are applied at the inflow, lateral and upper, and outflow boundaries, respectively. On the surfaces of the cube and the ground surface, no-slip conditions are imposed. In the present study, the Reynolds number is Re $(= Uh / \nu) = 10^4$, where h is the length of a side of the cube (height) and U is the wind speed at height h at the inflow boundary. The time step is set to $\Delta t = 2.0$
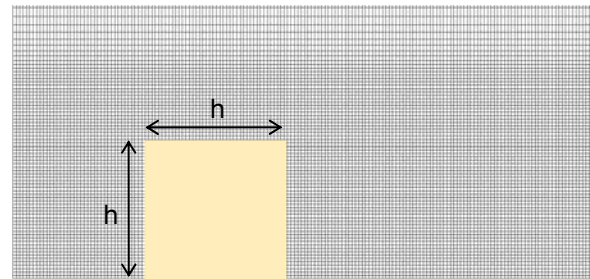

Fig.2 Computational grid in the vicinity of the cube from the simulation with RIAM-COMPACT®, structured grid, central plane (y = 0) normal to the spanwise (y) axis

(a) Side view (y = 0), overall view

(b) Side view (y = 0), enlarged view

(c) Top view (z = 0.5h), overall view
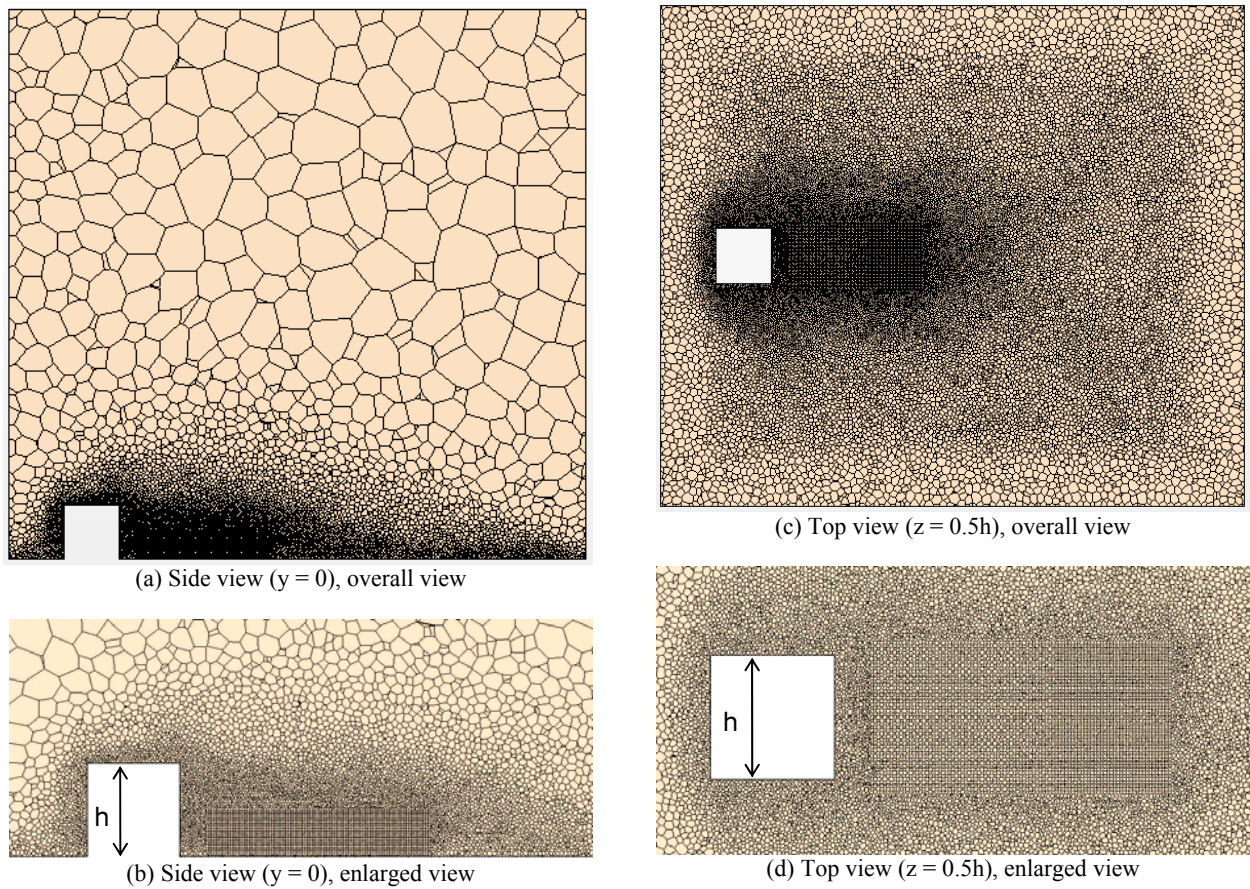

(d) Top view (z = 0.5h), enlarged view

Fig.3 Computational grid used for the simulation with STAR-CCM+, unstructured grid

$\times 10^{-3}$ (h / U) for the simulation with RIAM-COMPACT®. In contrast, the time step is set to $\Delta t = 2.5 \times 10^{-2}$ (h / U) for the simulation with STAR-CCM+.

Fig.2 shows the computational grid (structured grid) used for the simulation with RIAM-COMPACT®. The number of grid points used for this simulation are 326 (x) × 226 (y) × 67 (z) points (approximately 5 million points in total). The grid points in the x- and y-directions are spaced at an even interval of 0.04h, and the grid points in the z-direction are spaced at uneven intervals ranging from 0.003h to 0.6h.

For comparison, Fig.3 shows the computational grid (unstructured grid) used for the simulation with STAR-CCM+. The total number of grid points is approximately 1.5 million (1/3 of that used for the simulation with RIAM-COMPACT®). The grid resolution in the vicinity of the cube in the simulation with STAR-CCM+ is set to be nearly identical to that with RIAM-COMPACT®.

Tables 2 and 3 list the turbulence models (RANS and LES models) considered in the present comparative study. For convenience, simulations performed with the use of each of the

models are referred to as Cases 1 to 5. The models considered in the present study are the same as those from the previous study[1, 2]. A brief description of the WALE model in Case 4 is as follows: the WALE model has been

RANS models	**Case 1**	Spalart-Allmaras one-equation eddy-viscosity turbulence model: steady RANS
	Case 2	SST k-ω two-equation eddy -viscosity model: unsteady RANS (URANS)
LES models	**Case 3**	Standard Smagorinsky model: LES
	Case 4	WALE model: LES

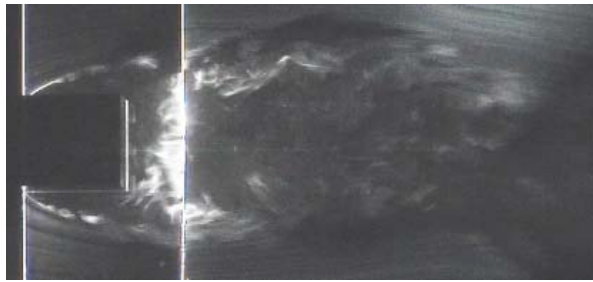Table 2 Turbulence models
used in the simulations with STAR-CCM+

LES model	**Case 5**	Standard Smagorinsky model: LES

Table 3 Turbulence model
used in the simulation with RIAM-COMPACT®

⟹ Flow
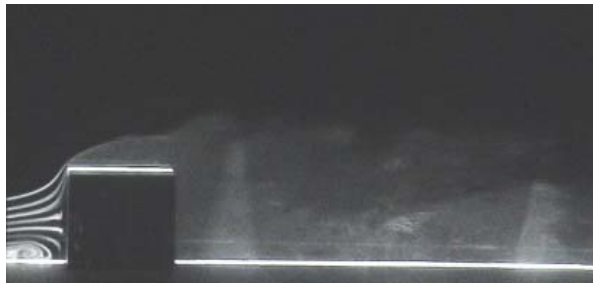
(a) Side view (y = 0)

(b) Top view (z = 0.5h), where h is the height of the cube

Fig.4 Wind tunnel experiment, flow visualization
by the smoke-wire method, instantaneous field

designed in such a way that 1) the eddy viscosity coefficient becomes zero in the vicinity of the ground surface without the use of a wall damping function and 2) the eddy viscosity coefficient is not calculated for laminar shear flow.

6. Simulation Results and Discussions

First, flow patterns generated in the vicinity of the cube considered in the present study are described based on photographs acquired during a wind tunnel experiment (smoke-wire method) (Fig.4). Both the vertical and horizontal cross-sections of the flow field (Figs.4(a) and 4(b), respectively) show that the shear layer which separates from the upstream, upper corners of the cube rolls up into isolated vortices. These isolated vortices then form into large-scale vortices, which are periodically shed downstream of the cube and then advance downstream. As a result, a three-dimensional, complex turbulent flow field is generated in the vicinity of the cube.

Figs.5 to 8 show comparisons of the simulation results. The time-averaged flow field and the turbulence statistics for Case 5 in these figures (RIAM-COMPACT® with the LES model) were evaluated from the time period t = 100 - 200 (h / U), during which the flow field was fully developed.

Subsequently, comparisons of the visualized flow fields in Figs.5 and 6 are discussed. Due to space limitations, these figures compare only the simulation results from Case 1 (STAR-CCM+ with the steady RANS model; a steady simulation in which the steady-state solution is obtained by using the number of time steps specified in Table 1 for time marching) and Case 5 (RIAM-COMPACT® with the LES model) as an example. An examination of Figs.5 and 6 reveals the following result: although a complex turbulent flow field is generated in the vicinity of the cube as was described for Fig.4, no significant difference exists between the results from the simulation which uses the RANS model (steady) and those from the simulation which uses the LES model (the standard Smagorinsky model). That is, the overall trends of the results are nearly the same between the two cases.

Figs.7 and 8 show comparisons of various turbulence statistics acquired with the use of the turbulence models considered for comparisons in the present study (RANS and LES models) (Tables 2 and 3). The turbulence statistics were evaluated at the positions x = -1h, 0h, +1h, and +3h. The figures also include the turbulence statistics acquired from a wind tunnel experiment previously conducted by the author. Comparisons of the profiles of the mean streamwise (x) velocity (Fig.7) reveal that the profiles vary at x = +3h in association with the use of different turbulence models, however, they generally resemble one another at the other positions (x = -1h, 0h, and +1h), independent of the turbulence model used. Comparisons of the standard deviation of the streamwise (x) velocity (Fig.8) show that no significant non-zero values were output at any of the positions when using the RANS models, as was the case in the previous study [1, 2]. In contrast, the simulations with the LES models reveal similar trends for the standard deviation of the streamwise (x) velocity for both the simulations with STAR-CCM+ (the standard Smagorinsky model and the WALE model) and with RIAM-COMPACT® (the standard Smagorinsky model).

Regarding the computational time, although the number of grid points used for the simulation with RIAM-COMPACT® (structured grid, approximately 5 million points) was approximately three times as large as that used for the simulations with STAR-CCM+ (unstructured grid, approximately 1.5 million points), the simulation with RIAM-COMPACT® completed much faster than those with STAR-CCM+, as was the case in the previous study [1, 2].
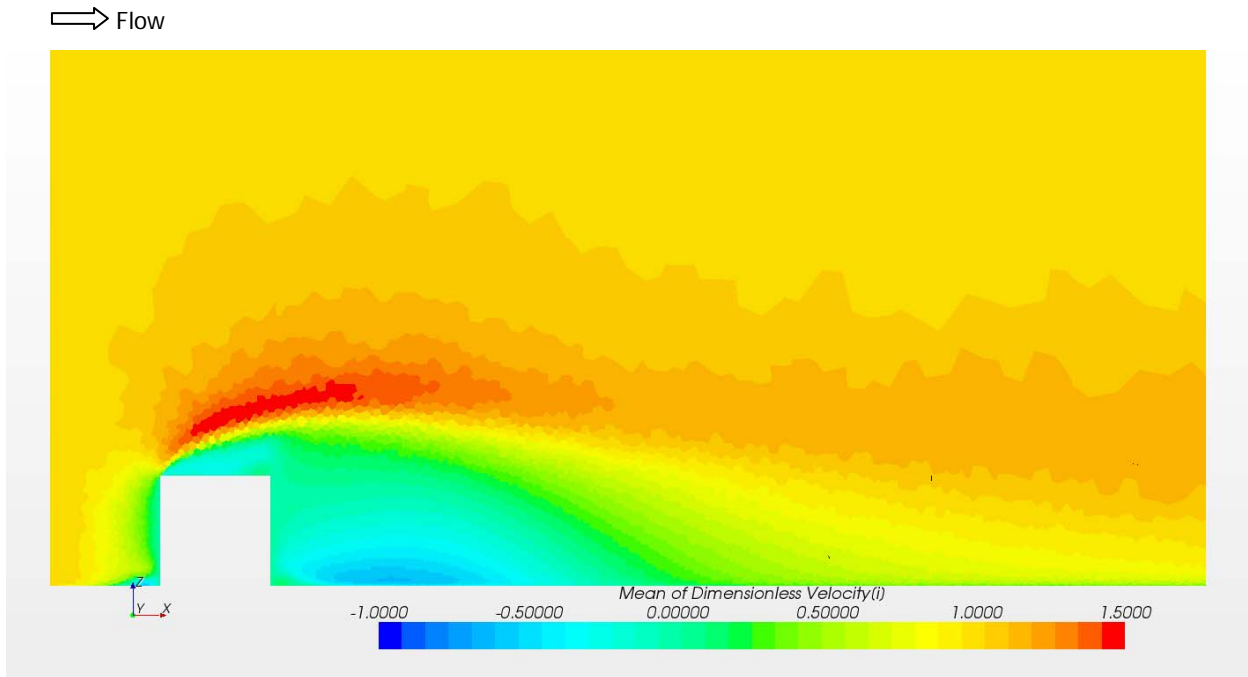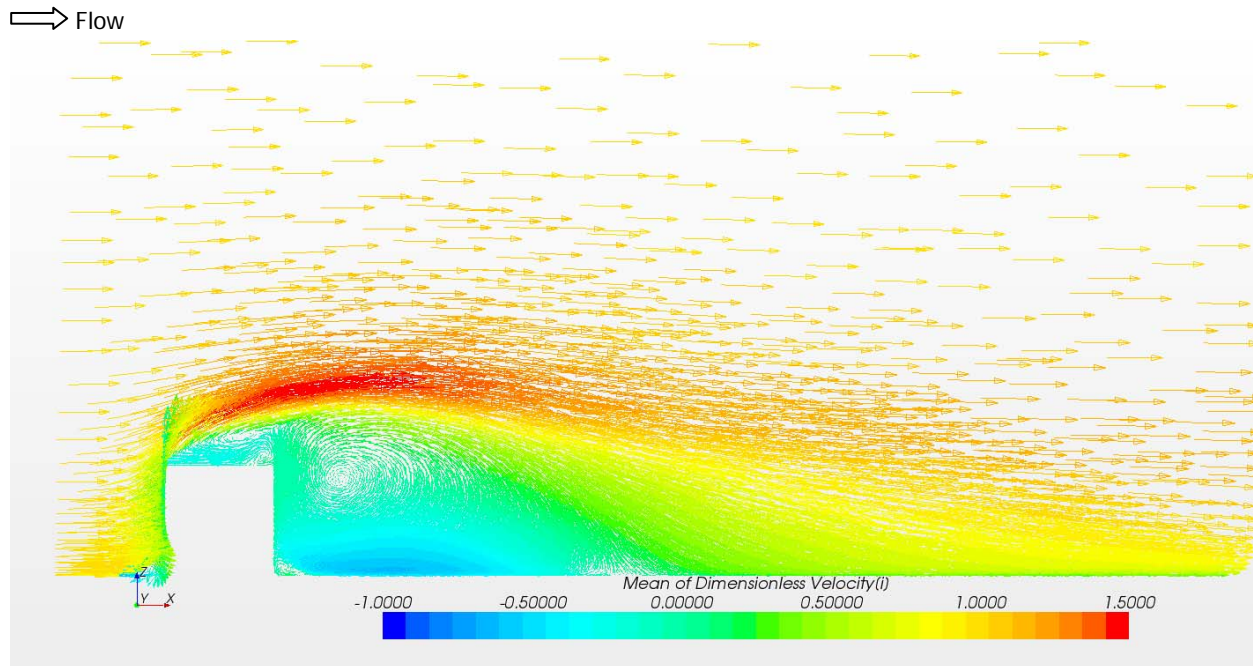
(a) Case 1, Simulation results from STAR-CCM+ with the use of the steady RANS model,
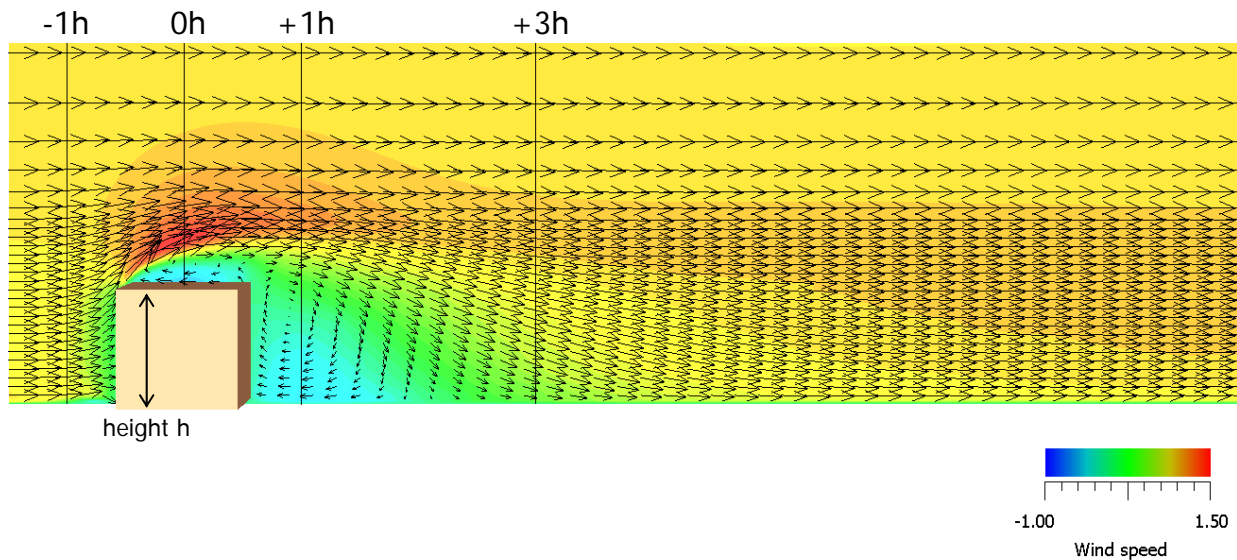Spalart-Allmaras one-equation eddy-viscosity turbulence model
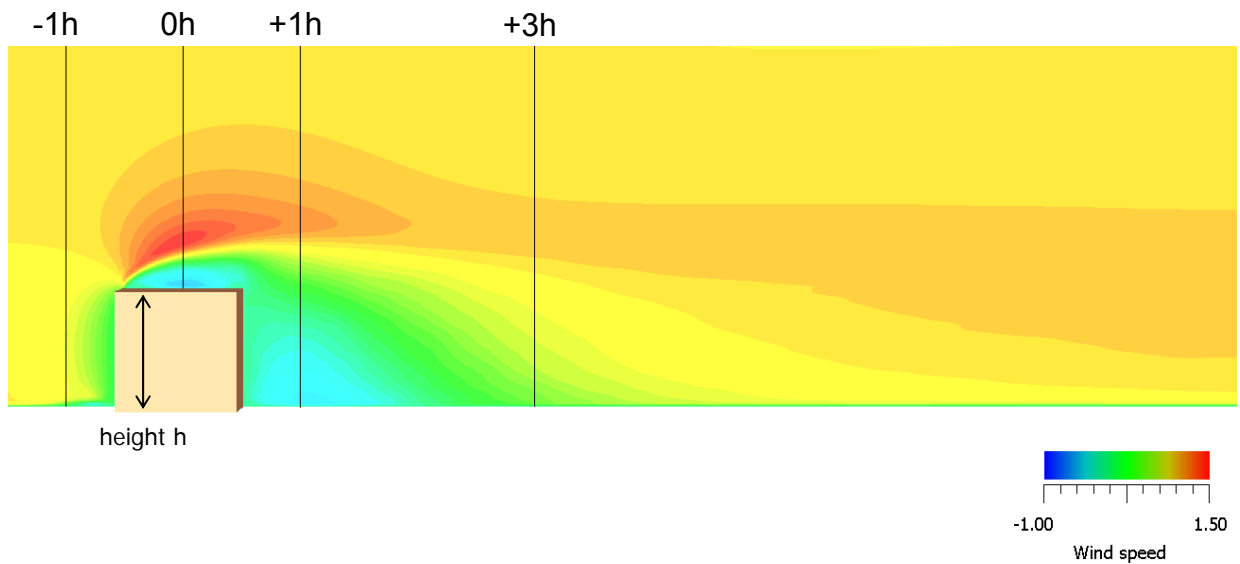
(b) Case 5, Simulation results from RIAM-COMPACT® with the use of the LES model,
standard Smagorinsky model, time-averaged field

Fig.5 Comparison of the streamwise (x) velocity component distribution,
central plane (y = 0) normal to the spanwise (y) axis.
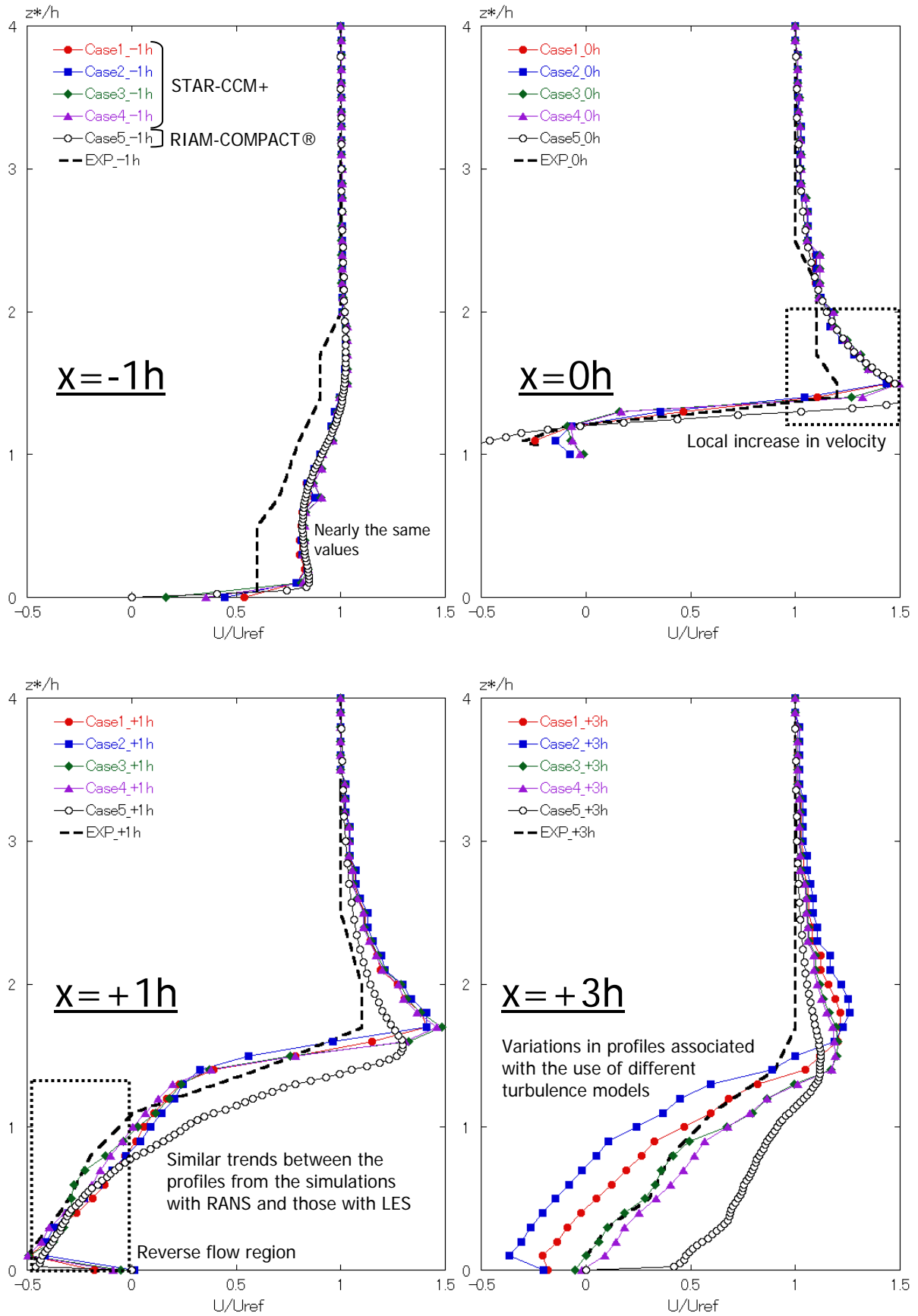Here, the velocity component is normalized by the magnitude of the uniform inflow wind velocity.

(a) Case 1, Simulation results from STAR-CCM+ with the use of the steady RANS model,
Spalart-Allmaras one-equation eddy-viscosity turbulence model

(b) Case 5, Simulation results from RIAM-COMPACT® with the use of the LES model,
standard Smagorinsky model, time-averaged field

Fig.6 Comparison of velocity vectors, central plane (y = 0) normal to the spanwise (y) axis.
Here, the velocity component is normalized by the magnitude of the uniform inflow wind velocity.

Fig. 7 Comparison of the mean streamwise (x) velocity profiles.
Here, the velocity component is normalized by the upper-air wind velocity above the location of each profile evaluation.
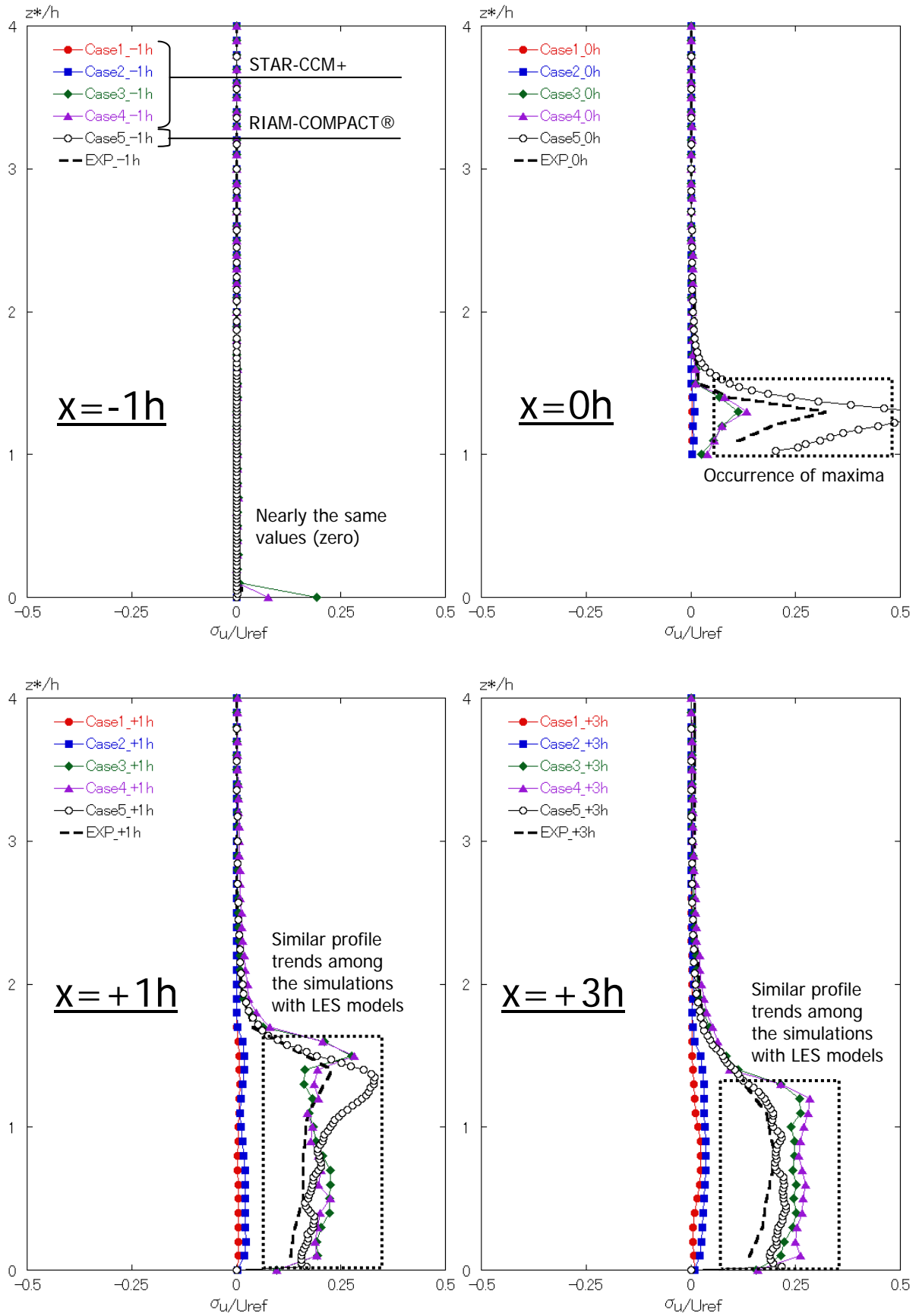
Fig.8 Comparison of the standard deviation of the streamwise (x) velocity.
Here, the velocity component is normalized by the upper-air wind velocity above the location of each profile evaluation.

7. Conclusion

In the previous paper [1, 2], the simulation results from RIAM-COMPACT® natural terrain version of airflow around an isolated-hill with a steep slope angle were compared to those from another commercially available CFD software.

In the present paper, in order to examine the prediction accuracy of RIAM-COMPACT® (turbulence model: the standard Smagorinsky LES model), developed by the author's research group, the simulation results from RIAM-COMPACT® of airflow around a three-dimensional cube were compared to those from one of the leading software packages, STAR-CCM+. For the simulations with STAR-CCM+, both RANS and LES turbulence models were adopted. Specifically, for the RANS turbulence model, two such models were selected for use: the Spalart-Allmaras one-equation eddy-viscosity model (steady RANS) and the SST k-ω two-equation eddy-viscosity model (unsteady RANS). Similarly, for the LES turbulence model, two such models were selected for use: the standard Smagorinsky model and the WALE model.

The comparisons of the simulation results from the use of the four turbulence models revealed the following findings. Comparisons of the visualized large-scale flow fields showed no significant differences between the simulation results from the use of the RANS turbulence models (i.e., steady and unsteady RANS models) and those from the use of the LES models (i.e., the standard Smagorinsky model and the WALE model) despite the generation of a complex turbulent flow field in the vicinity of the cube. The overall trends of the visualized flow field were nearly the same among all the simulations.

Comparisons of the mean streamwise (x) velocity profiles revealed variations in the velocity at x = +3h, associated with the use of different turbulence models. However, at other positions (x = -1h, 0h, and +1h), the velocity profiles generally resembled one another, independent of the turbulence model used in each simulation. As for the standard deviation of the streamwise (x) velocity, no significant non-zero values were output with the use of the RANS models at any of the positions, as was the case in the previous study [1, 2]. The simulations with the LES models revealed that the trends of this variable were similar among the simulations with STAR-CCM+ (the standard Smagorinsky model and the WALE model) and RIAM-COMPACT® (the standard Smagorinsky model).

Regarding the computational time, although the number of grid points used for the simulation with RIAM-COMPACT® was approximately three times as large (structured grid, approximately 5 million grid points) as that used for the simulations with STAR-CCM+ (unstructured grid, approximately 1.5 million grid points), the simulation with RIAM-COMPACT® completed much faster than those with STAR-CCM+, as was the case in the previous study [1,2].

References

1) Takanori UCHIDA, Reproducibility of Complex Turbulent Flow Using Commercially-Available CFD Software –Report 1: For the Case of a Three-Dimensional Isolated-Hill With Steep Slopes–, Reports of RIAM, Kyushu University, No.150, in press, 2016

2) Takanori UCHIDA, Reproducibility of Complex Turbulent Flow Using Commercially-Available CFD Software –Report 2: For the Case of a Two-Dimensional Ridge With Steep Slopes–, Reports of RIAM, Kyushu University, No.150, in press, 2016

Appendix

In order to compare the results of the simulation with RIAM-COMPACT® (turbulence model: the standard Smagorinsky LES model) and those from the wind tunnel experiment previously conducted by the author more closely, an additional simulation was performed with RIAM-COMPACT®, in which the computational domain upstream of the cube was extended. Fig.9 shows the computational domain used in this simulation. Figs.10 - 12 show the simulation results. Both Figs.11 and 12 indicate that RIAM-COMPACT® (turbulence model: the standard Smagorinsky LES model), with the use of the extended computational domain, successfully reproduced the flow field from the wind tunnel experiment..
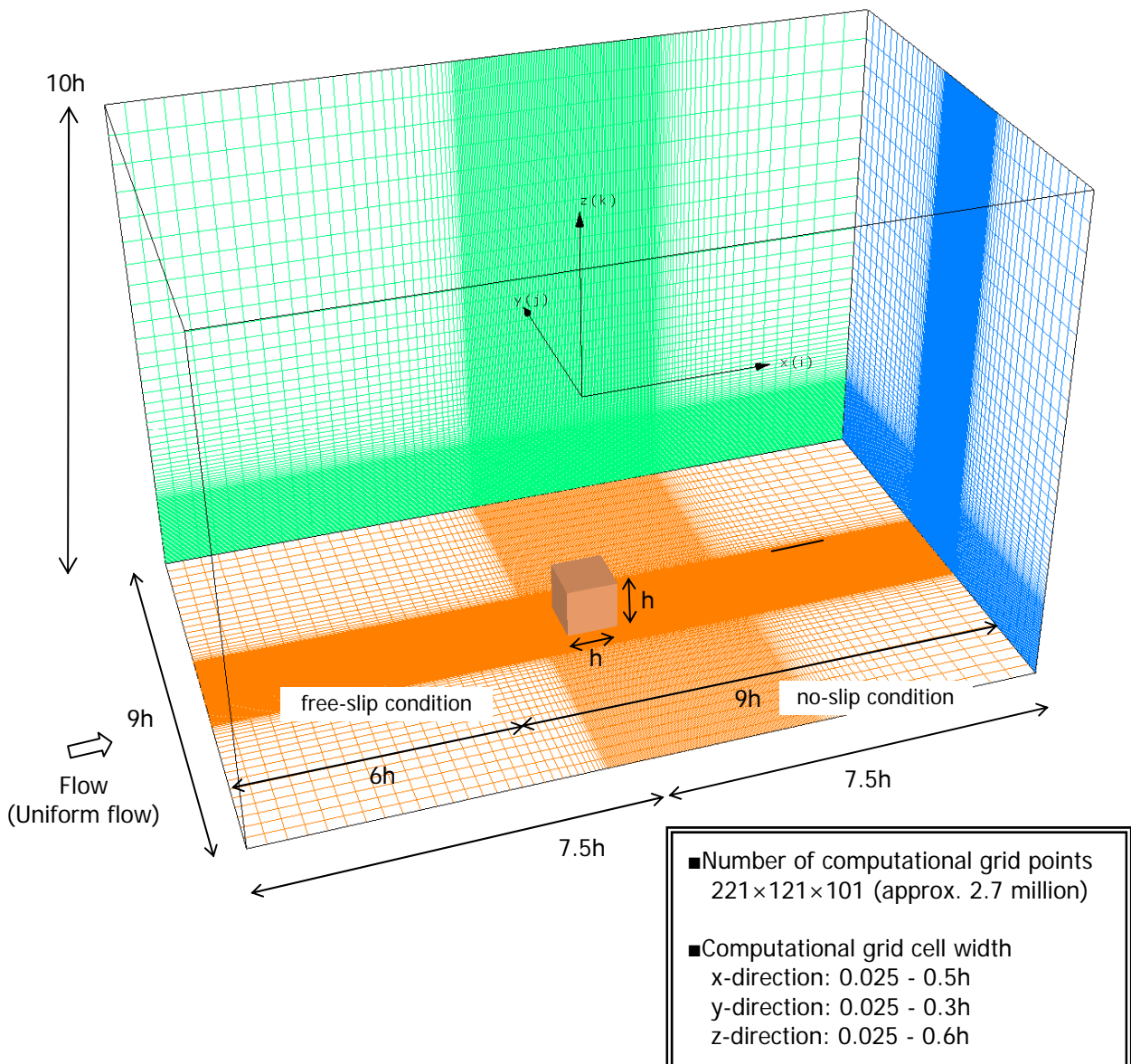

Fig.9 Computational domain geometrically similar to the set-up from the wind tunnel experiment, boundary conditions identical to those in Fig.1 except as shown for the ground surface.
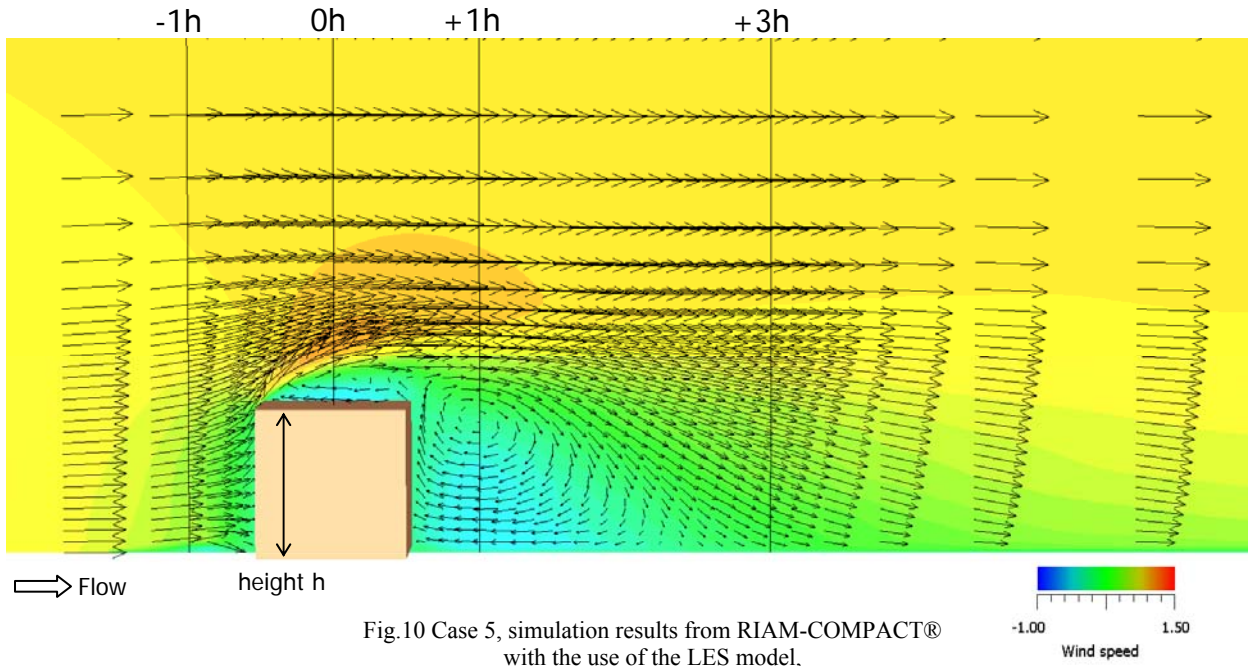
Fig.10 Case 5, simulation results from RIAM-COMPACT®
with the use of the LES model,
the standard Smagorinsky model, time-averaged field

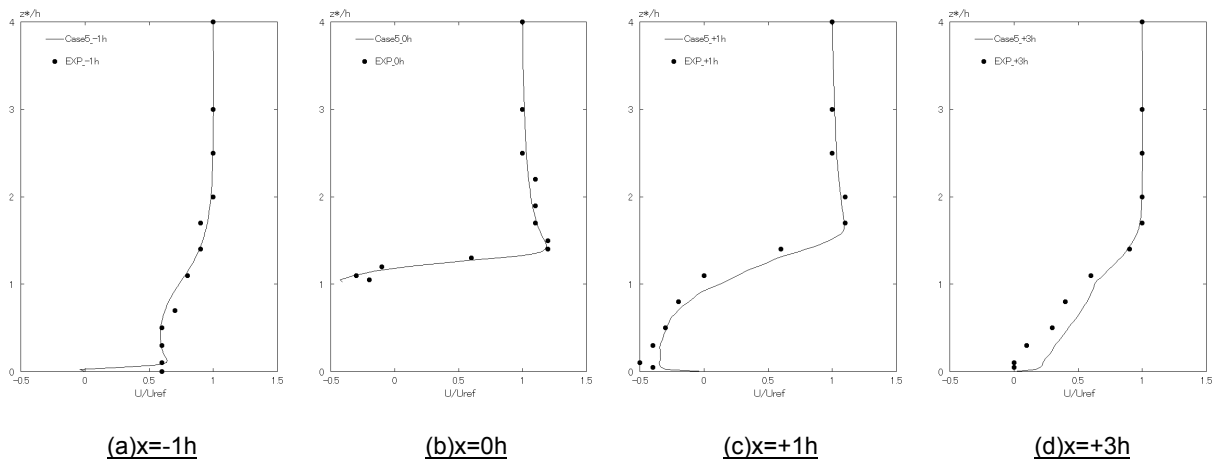(a)x=-1h   (b)x=0h   (c)x=+1h   (d)x=+3h

Fig.11 Comparison of the mean streamwise (x) velocity profiles,
filled circle: wind tunnel experiment, line: simulation with RIAM-COMPACT® (turbulence model: LES)

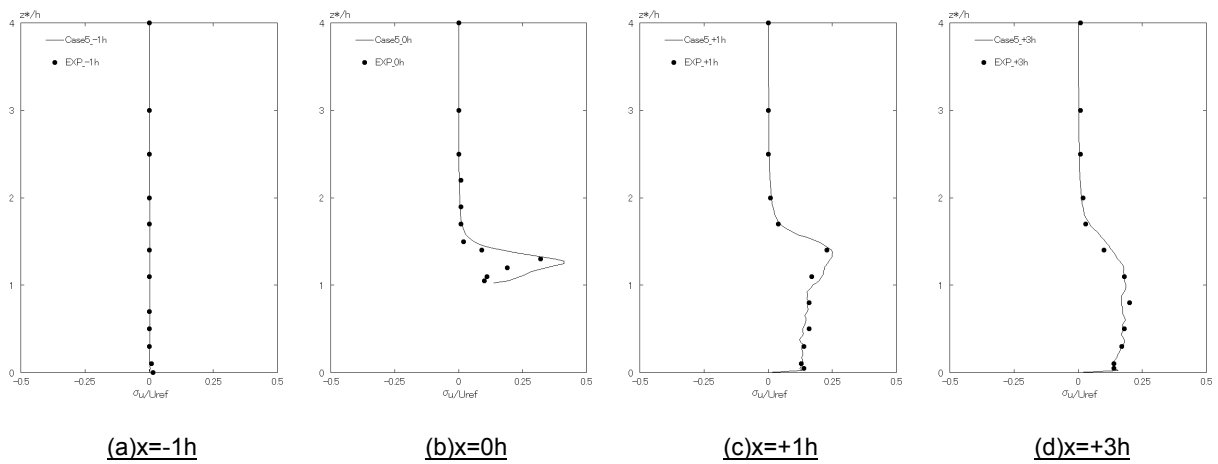(a)x=-1h   (b)x=0h   (c)x=+1h   (d)x=+3h

Fig.12 Comparison of the standard deviation of the streamwise (x) velocity,
filled circle: wind tunnel experiment, line: simulation with RIAM-COMPACT® (turbulence model: LES)